

Heterolytic Activation of Dihydrogen at Transition-Metal Sulfur Sites in Coordinatively Unsaturated $[\text{Rh}(\text{L})(\text{“buS}_4\text{”})]\text{BF}_4$ Complexes, Involving Neutral Hydrides, Thiol Hydrides, and Thiol–Hydride Proton Scrambling (L = CO, PCy_3 ; “buS₄”²⁻ = 1,2-Bis[(2-mercapto-3,5-di-*tert*-butylphenylthio)ethane²⁻])**

Dieter Sellmann,* Gabriele H. Rackelmann, and Frank W. Heinemann

Dedicated to Professor Hartmut Bärnighausen on the occasion of his 65th birthday

Abstract: $[\text{Rh}(\text{H})(\text{L})(\text{“buS}_4\text{”})]$ complexes (L = CO (**1**), PCy_3 (**2**); “buS₄”²⁻ = 1,2-bis[(2-mercapto-3,5-di-*tert*-butylphenylthio)ethane²⁻]) catalyze the D_2/H^+ exchange between D_2 and EtOH protons in the presence of catalytic amounts of Brønsted acids. A mechanism and complete cycle for the heterolytic D_2 cleavage are proposed that are based on characterization of key intermediates and monitoring of key reactions. The key intermediates are the thiol hydride complexes $[\text{Rh}(\text{H})(\text{L})(\text{“buS}_4\text{”}-\text{H})]\text{BF}_4$, L = CO (**3**), PCy_3 (**4**), the coordinatively unsaturated complexes $[\text{Rh}(\text{L})(\text{“buS}_4\text{”})]\text{BF}_4$, L = CO (**5**), PCy_3 (**6**), which are the actual catalysts, and the deuterium-labeled derivatives of **1–4**. Complexes **3** and **4** form from **1** and **2** by protonation with HBF_4 , and they release H_2 to give **5** and **6**. Complex **5** dimerizes in the solid state and was

characterized by X-ray structure determination of $5 \cdot 8\text{CH}_2\text{Cl}_2$ (triclinic space group $P\bar{1}$, $a = 1048.2(4)$ pm, $b = 1430.0(5)$ pm, $c = 1785.7(7)$ pm, $\alpha = 100.49(3)^\circ$, $\beta = 102.92(3)^\circ$; $\gamma = 103.68(3)^\circ$, $Z = 1$). Complex **6** is mononuclear and adds H_2O or THF reversibly to give the highly labile $[\text{Rh}(\text{L})(\text{PCy}_3)(\text{“buS}_4\text{”})]\text{BF}_4$, L = H_2O (**7**), THF (**8**). CO is irreversibly added to give the stable $[\text{Rh}(\text{CO})(\text{PCy}_3)(\text{“buS}_4\text{”})]\text{BF}_4$ (**9**), whose high-frequency $\nu(\text{CO})$ (2081 cm^{-1}) indicates a relatively low electron density at the Rh center. Complex **6** also adds to H_2 to give **4**,

which can be deprotonated by solid Na_2CO_3 or H_2O to yield neutral **2**. ^1H NMR and ^2H NMR spectroscopy revealed the scrambling of thiol protons and hydride ligands in **3** and **4** and its deuterium-labeled derivatives. This exchange of thiol protons for hydride ligands is explained by a transient $[\text{Rh}(\eta^2\text{-H}_2)]$ species. Low-temperature $^1\text{H}/^2\text{H}$ NMR spectroscopy showed that protonation of **2** yields four diastereomers of **4** resulting from protonation of the four stereochemically nonequivalent lone pairs at the thiolate donors of **2**. The relevance of these findings to H_2 activation at transition-metal sulfur sites in hydrogenases or hydrotreatment catalysts, and differences from the H_2 cleavage achieved with other complexes not containing “built-in” Brønsted-basic centers, are discussed.

Keywords

dihydrogen activation · heterolytic cleavage · hydrido complexes · rhodium · S ligands

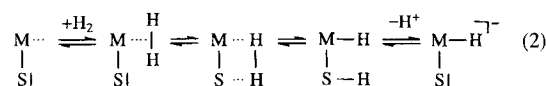
Introduction

Activation of H_2 by transition-metal complexes can occur by homolytic or heterolytic cleavage of the H–H bond.^[1] Homolysis is usually achieved by low-valent metal complexes whose metal centers have an increased oxidation state after homolysis. Heterolysis, that is, the splitting of H_2 into a proton and a

hydride ion, takes place at metal centers in medium or high oxidation states and requires the assistance of Brønsted bases. Catalytic H_2 heterolysis is a reactivity feature of hydrogenases, which catalyze the redox equilibrium [Eq. (1 a)] and the D_2/H^+ exchange reaction [Eq. (1 b)].^[2, 3] These reactions are assumed



to take place at the metal sulfur sites of hydrogenases.^[4] Equation (2) suggests a mechanism for the heterolytic cleavage. This



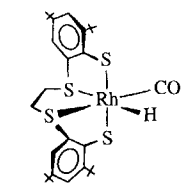
[*] Prof. Dr. D. Sellmann, Dr. G. H. Rackelmann, Dr. F. W. Heinemann
Institut für Anorganische Chemie der Universität Erlangen–Nürnberg
Egerlandstr. 1, D-91058 Erlangen (Germany)
Fax: Int. code + (9131) 857-367
e-mail: sellmann@anorganik.chemie.uni-erlangen.de

[**] Transition-Metal Complexes with Sulfur Ligands, Part 128. Part 127: D. Sellmann, T. Gottschalk-Gaudig, F. W. Heinemann, *Inorg. Chim. Acta*, in press.

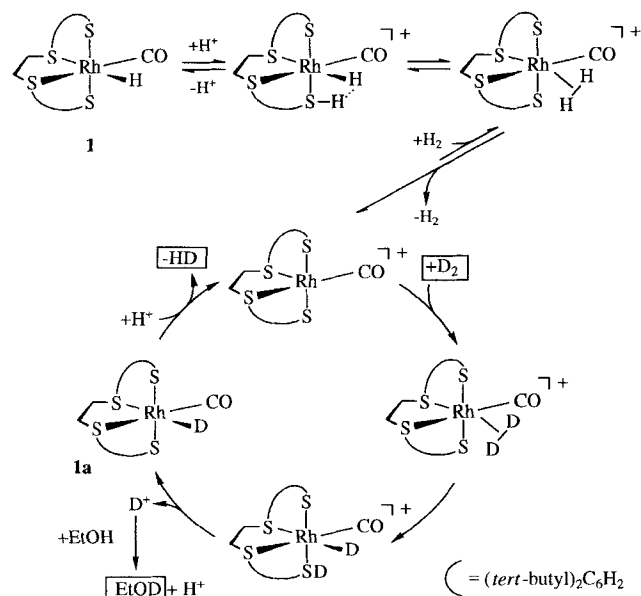
comprises the binding of H_2 to a vacant coordination site on the active center, and the subsequent heterolysis of H_2 by the concerted attack of the Lewis-acidic metal and the Brønsted-basic sulfur site. Coordinatively unsaturated complexes, η^2-H_2 , thiol hydride, and hydride complexes have been proposed as key intermediates.^[1, 5] The mechanism according to Equation (2) is plausible, but has never been proved in detail.

Dihydrogen activation by transition-metal sulfur sites is also a key feature of hydrotreatment catalysts based on transition-metal sulfides. Hydrotreatment of petroleum is a high-temperature and high-pressure process.^[6] The detection of SH groups on the surface of the heterogeneous catalysts^[7] possibly indicates mechanistic relations between the high-temperature hydrotreatment and the low-temperature hydrogenase reactions.

Detailed insights into the mechanisms of hydrogenase and/or hydrotreatment reactions can be expected from transition-metal complexes that exhibit sulfur-rich coordination spheres and make it possible to trap key intermediates. Such complexes are extremely rare;^[8] one example is the rhodium complex $[Rh(H)(CO)(\text{“}^{\text{bu}}S_4\text{”})]$ (**1**).^[9] In the presence of catalytic amounts of Brønsted acids such as hydrochloric acid, **1** catalyzes the D_2/H^+ exchange according to Equation (1 b), and it yields the deuterium derivative $[Rh(D)(CO)(\text{“}^{\text{bu}}S_4\text{”})]$ (**1a**) from **1** and D_2 . These observations led to the suggestion of the reaction cycle for the D_2/H^+ exchange shown in Scheme 1.^[9]



$[Rh(H)(CO)(\text{“}^{\text{bu}}S_4\text{”})]$ (**1**)



Scheme 1. D_2/H^+ exchange catalyzed by $[Rh(H)(CO)(\text{“}^{\text{bu}}S_4\text{”})]$ (**1**) in the presence of catalytic amounts of hydrochloric acid.

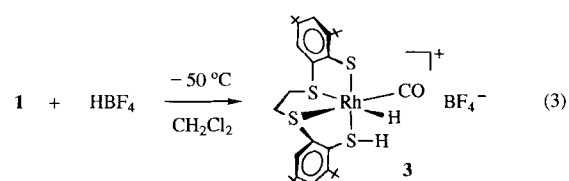
With respect to the transition-metal sulfur site and D_2/H^+ exchange catalysis, **1** combines structural and functional features of hydrogenase centers. Important key intermediates of the catalytic cycle, however, have not yet been identified. These are, in particular, the thiol hydride species $[Rh(H)(CO)(\text{“}^{\text{bu}}S_4\text{”}-H)]^+$ and the coordinatively unsaturated $[Rh(CO)(\text{“}^{\text{bu}}S_4\text{”})]^+$, which is the actual catalyst for the heterolytic cleavage of the D_2

molecule. The investigations described here were aimed at the unambiguous proof of the existence of these species. The recent isolation of the PCy_3 derivative $[Rh(H)(PCy_3)(\text{“}^{\text{bu}}S_4\text{”})]$,^[10] which is less labile than **1** and accessible from **1** and PCy_3 , made it possible substantially to corroborate the mechanism of Scheme 1.

Results

Protonation of $[Rh(H)(L)(\text{“}^{\text{bu}}S_4\text{”})]$ and characterization of the resultant thiol complexes: Treatment of the hydrido complex $[Rh(H)(CO)(\text{“}^{\text{bu}}S_4\text{”})]$ (**1**) and its PCy_3 derivative $[Rh(H)(PCy_3)(\text{“}^{\text{bu}}S_4\text{”})]$ (**2**) dissolved in CH_2Cl_2 with 1 equiv of HBF_4 in Et_2O resulted in protonation of the thiolate donors. The resultant hydrido thiol complexes $[Rh(H)(CO)(\text{“}^{\text{bu}}S_4\text{”}-H)]BF_4$ (**3**) and $[Rh(H)(PCy_3)(\text{“}^{\text{bu}}S_4\text{”}-H)]BF_4$ (**4**) both proved highly labile and will be described separately.

Protonation of **1 by HBF_4 :** The formation of the very temperature-labile yellow $[Rh(H)(CO)(\text{“}^{\text{bu}}S_4\text{”}-H)]BF_4$ (**3**) according to Equation (3) could be monitored only at temperatures below



$-40^\circ C$. Above this temperature, **3** rapidly decomposed. IR monitoring showed that the $\nu(CO)$ band of **1** (2079 cm^{-1}) was replaced by the $\nu(CO)$ band of **3** (2110 cm^{-1}) (Figure 1). The frequency shift of 31 cm^{-1} corresponds with the $\nu(CO)$ shifts

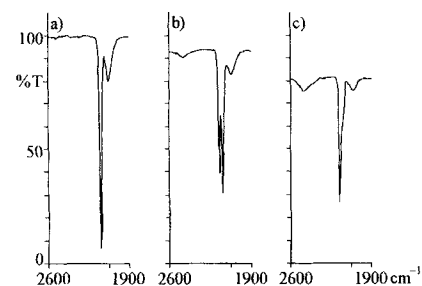


Figure 1. IR spectra of CH_2Cl_2 solutions (at $-70^\circ C$) of a) $[Rh(H)(CO)(\text{“}^{\text{bu}}S_4\text{”})]$ (**1**), b) **1** after addition of 0.5 equiv of HBF_4 , and c) **1** after addition of 1 equiv of HBF_4 in CH_2Cl_2 .

observed for $[Fe(CO)_2(\text{“}S_4\text{”})]$ or $[Fe(CO)(\text{“}N_H S_4\text{”})]$ ($\text{“}S_4\text{”}^{2-} = 1,2\text{-bis}(2\text{-mercaptophenylthio)ethane}^{2-}$, $\text{“}N_H S_4\text{”}^{2-} = 2,2'\text{-bis}(2\text{-mercaptophenylthio)diethylamine}^{2-}$) upon protonation or alkylation of their thiolate donors.^[11] The relatively weak and broad $\nu(RhH)$ of **1** at 2003 cm^{-1} was replaced by the $\nu(RhH)$ of the resultant **3** at 1992 cm^{-1} . The $\nu(SH)$ bond of **3** was detected at 2482 cm^{-1} . Evaporating the reaction solution to dryness led to partial decomposition of **3** even at $-50^\circ C$.

Monitoring of the reaction according to Equation (3) by low-temperature ($\sim -50^\circ C$) 1H NMR spectroscopy showed that all

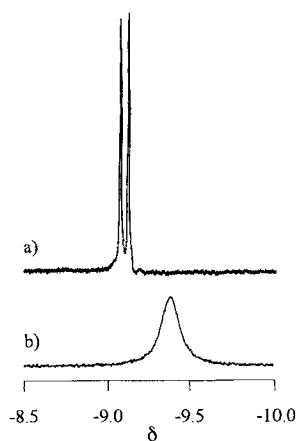
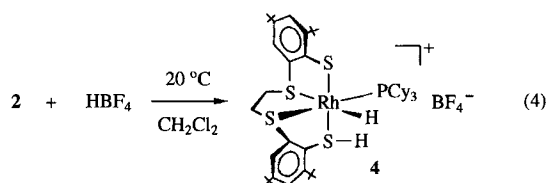


Figure 2. Hydride resonances in the ^1H NMR spectra of a) $[\text{Rh}(\text{H})(\text{CO})(\text{tBuS}_4)]$ (**1**) and b) $[\text{Rh}(\text{H})(\text{CO})(\text{tBuS}_4\text{-H})]\text{BF}_4$ (**3**) in CD_2Cl_2 at -50°C .

CH signals of **1** were replaced by new signals indicating the quantitative formation of **3**. (The *tert*-butyl groups and the four aromatic protons of the “ tBuS_4 ” $^{2-}$ ligand in $[\text{M}(\text{L}_1)(\text{L}_2)(\text{tBuS}_4)]$ complexes are particularly sensitive probes for monitoring reactions by ^1H NMR spectroscopy.^[9, 10]) The characteristic hydride doublet of **1** at $\delta = -9.44$ ($^1J(\text{RhH}) = 12.8$ Hz) changed to a broad unresolved signal at $\delta = -9.38$ (Figure 2). Signals arising from SH groups were not detected at -50°C . The reason is certainly the broadness of the SH signal due to exchange processes which are described below for the variable-temperature experiments with the $[\text{Rh}(\text{H})(\text{PCy}_3)(\text{tBuS}_4)]$ derivative **2**. It proved impossible to investigate these assumed exchange processes with **3** by temperature-dependent ^1H NMR spectra, because decreasing the temperature below -50°C resulted in precipitation of **3**, whereas raising the temperature above -40°C led to decomposition of **3**. However, the possibility that the signal at $\delta = -9.38$ resulted from formation of a $\eta^2\text{-H}_2$ complex was excluded. The signal intensity corresponded to one proton only. In addition, T_1 time measurements at -50°C resulted in $T_1 = 2300$ ms, which is typical of η^1 -hydride ligands and usually much too large for $\eta^2\text{-H}_2$ complexes.^[14, 12–14]

Protonation of $[\text{Rh}(\text{H})(\text{PCy}_3)(\text{tBuS}_4)]$ (2**):** The hydride complex **2** is significantly less labile than **1**. The same holds for its protonated product **4**, which could be obtained in solution at room temperature [Eq. (4)].



Addition of HBF_4 (in Et_2O) to CH_2Cl_2 solutions of **2** at room temperature resulted in a color change from yellow to dark red. The IR spectra of these solutions exhibited a medium intensity band at 2459 cm^{-1} , assigned to $\nu(\text{SH})$. The $\nu(\text{RhH})$ band was observed at 2032 cm^{-1} and is slightly shifted compared with that of **2** in KBr (2040 cm^{-1}). Although it was less labile than **3**, **4** also decomposed slowly in solution, as indicated by the diminution of the IR bands over a period of 1–2 h. Removal of the CH_2Cl_2 solvent by evaporation resulted in a color change from red to deep violet. The remaining residue was characterized as $[\text{Rh}(\text{PCy}_3)(\text{tBuS}_4)]\text{BF}_4$ (**6**) (see below).

The ^1H NMR spectrum of **4** recorded at $+30^\circ\text{C}$ in CD_2Cl_2 resembles that of **3** in CD_2Cl_2 at -50°C . In addition to the

characteristic $[\text{Rh}(\text{PCy}_3)(\text{tBuS}_4)]$ signals indicating C_1 symmetry, the ^1H NMR spectrum of **4** exhibits a broad signal at $\delta = -10.40$ and an extremely broad signal at $\delta \approx 5.5$. The $\delta = -10.40$ signal is slightly shifted when compared with the pseudo-triplet hydride signal of **2** at $\delta = -11.02$ (Figures 3a and 3b).

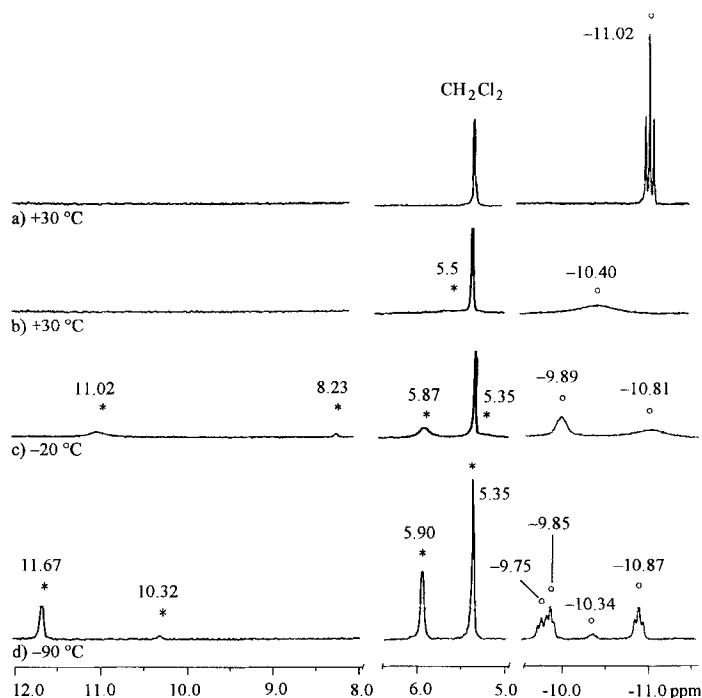


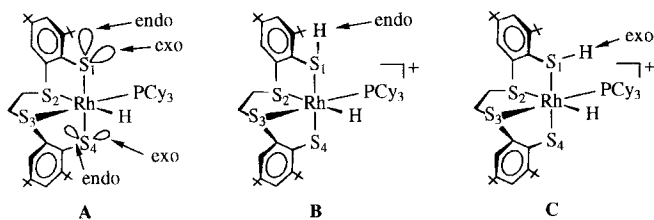
Figure 3. Details of the ^1H NMR spectra of a) $[\text{Rh}(\text{H})(\text{PCy}_3)(\text{tBuS}_4)]$ (**2**) (in CD_2Cl_2 at $+30^\circ\text{C}$) and $[\text{Rh}(\text{H})(\text{PCy}_3)(\text{tBuS}_4\text{-H})]\text{BF}_4$ (**4**) at b) $+30^\circ\text{C}$, c) -20°C , d) -90°C (in CD_2Cl_2) (* = SH resonances; $^{\circ}$ = RhH resonances).

The good solubility of **4** made it possible to record temperature-dependent ^1H NMR spectra down to -90°C . These revealed that the two broad signals at $\delta = -10.40$ and ≈ 5.5 split into four signals each. (Likewise, the signals of the aromatic protons and the *tert*-butyl groups split into complex multiplets upon cooling.) At -90°C , the spectrum depicted in Figure 3d results. The temperature dependence of the ^1H NMR spectra and the number, splitting, and intensity of the signals in Figure 3d suggest the following interpretation. The signals in the high-field region are assigned to RhH resonances. The splitting of these signals, which can be particularly well observed for the signal at $\delta = -10.87$, is due to $^1J(\text{RhH})$ and $^2J(\text{PH})$ couplings that lead to pseudo-triplets. Four of these pseudo-triplets can be detected. They have unequal intensities, and they indicate the presence of four diastereomeric hydride complexes in different amounts.

This interpretation is corroborated by the temperature dependence of the broad singlet at $\delta \approx 5.5$ (at $+30^\circ\text{C}$). This signal splits into four low-field signals in the range $\delta = 5\text{--}12$, which are assigned to SH resonances. The signal at $\delta = 5.35$ is isochronous with the solvent signal, but can be unequivocally recognized from the increase in intensity of this signal between the -20°C and -90°C spectra. The intensities of the four SH and four RhH resonances correlate and make it possible to conclude that four diastereomeric rhodium hydride thiol complexes are present. Integration of the respective signals (not

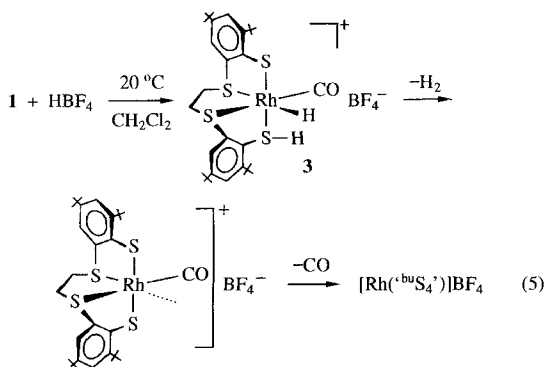
shown) gives a ratio of approximately 7:7:1:5 for these diastereomers.

The formation of four diastereomeric rhodium hydride thiol complexes is explained by the C_1 symmetry of $[\text{Rh}(\text{H})(\text{PCy}_3)(\text{S}_4^{\text{bu}})]$ (**2**) and the stereochemically inequivalent four lone pairs at the two thiolate donors (see structure **A**). It has been shown previously that these lone pairs can be distinguished by their *endo* or *exo* orientation towards the $[\text{M}(\text{L}_1)(\text{L}_2)(\text{S}_4^{\text{bu}})]$ core.^[15] Protonation of these four lone pairs results in four diastereomeric hydride thiol complexes, for example, structures **B** and **C**. Being diastereomeric, the hydride thiol complexes differ energetically, so they form in different yields. The ^1H NMR spectra reveal that the four diastereomers are interconverted, to an extent that depends on temperature.



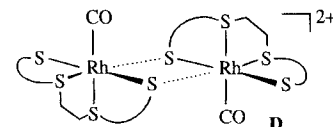
Characterization of the products resulting from decomposition of the hydride thiol complexes 3 and 4: Although to a different degree, the CH_2Cl_2 solutions of both **3** and **4** proved temperature-labile and released gas. The resultant products remaining in solution could be isolated and characterized.

When 1 equiv of HBF_4 was added to **1** in CH_2Cl_2 solution at room temperature, the solution immediately changed color from yellow to red and evolved ca. 1.8 equiv of gas. The gas was identified as a mixture of H_2 and CO by gas chromatography. The same reaction was observed when **1** in CH_2Cl_2 solution was treated with HBF_4 at -50°C and subsequently warmed to 20°C . Evaporation of the solution to dryness yielded a very dark red residue that exhibited low-intensity $\nu(\text{CO})$ IR bands of residual CO groups, but had no rhodium hydride signal in the ^1H NMR spectrum. These observations are compatible with reaction according to Equation (5). Complex **3**, resulting from

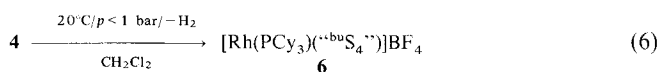


protonation of **1**, is unstable and releases H_2 . The resultant coordinatively unsaturated $[\text{Rh}(\text{CO})(\text{S}_4^{\text{bu}})]\text{BF}_4$ is also unstable, and releases CO , presumably to yield $[\text{Rh}(\text{S}_4^{\text{bu}})]\text{BF}_4$, which has not been characterized in detail.

The reaction sequence according to Equation (5) was corroborated by X-ray structure analysis of the binuclear $[\{\text{Rh}(\text{CO})(\text{S}_4^{\text{bu}})\}_2](\text{BF}_4)_2$ (**5**). Complex **5** was obtained in small amounts in the form of dark red single crystals from reaction solutions that had been stored at -30°C for one year. Complex **5** exhibits a core structure in which the dotted $\text{Rh}-\text{S}$ distances are significantly longer than the $\text{Rh}-\text{S}$ distances within the $[\text{Rh}(\text{CO})(\text{S}_4^{\text{bu}})]^+$ fragments indicated in structure **D**.

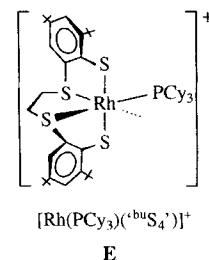


CH_2Cl_2 solutions of **4**, obtained according to Equation (4), proved significantly more stable than those of **3**. However, attempts to isolate **4** from these solutions by evaporating the CH_2Cl_2 led to a rapid color change from red to deep violet and resulted in a deep violet residue that was identified as $[\text{Rh}(\text{PCy}_3)(\text{S}_4^{\text{bu}})]\text{BF}_4$ (**6**). Its formation can be explained by a reaction between the hydride and thiol protons of **4** and subsequent release of H_2 according to Equation (6).



Complex **6** is readily soluble in common solvents except *n*-hexane, CCl_4 , and H_2O . It could be characterized by IR, ^1H , ^{31}P NMR, and mass spectroscopy, and by chemical reactions.

The spectroscopic properties and chemical reactivity indicate that **6** contains the C_1 symmetrical mononuclear and coordinatively unsaturated $[\text{Rh}(\text{PCy}_3)(\text{S}_4^{\text{bu}})]^+$ cation (**E**). For example, the mass spectrum of **6** exhibited the $[\text{Rh}(\text{PCy}_3)(\text{S}_4^{\text{bu}})]^+$ cation at $m/z = 915$ but no signals resulting from di- or polynuclear species. In the ^1H NMR spectrum of **6**, the four *tert*-butyl groups prove magnetically inequivalent and give rise to three signals in the ratio 2:1:1; the four aromatic protons appear as four singlets. The ^{31}P NMR spectrum shows one signal. Attempts to grow single crystals for an X-ray structural determination of **6** were unsuccessful, so solid-state dimerization of **6** cannot be ruled out completely. However, molecular models show that the steric demands of the $(\text{S}_4^{\text{bu}})^{2-}$ and PCy_3 ligands would strongly disfavor such a dimerization.



The stabilization of the vacant site in coordinatively unsaturated **6** can be traced back to steric shielding by the PCy_3 and $(\text{S}_4^{\text{bu}})^{2-}$ ligands and, in addition, to $\text{S}(\text{thiolate}) \rightarrow \text{Rh} \pi$ donation. Stabilization of vacant sites by $\text{S}=\text{M} \pi$ donation is documented for numerous coordinatively unsaturated 16-valence-electron complexes, for example $[\text{Cr}(\text{CO})_3(\text{S}_2\text{C}_6\text{H}_4)]^{2-}$ ^[16] or $[\text{Fe}(\text{N}_4\text{H}_4)]$.^[17] In **6**, the vacant site is possibly further stabilized by agostic $\text{Rh} \cdots \text{HC}(\text{cyclohexyl})$ interactions. In fact, the ^1H NMR multiplet of PCy_3 appears at room temperature in the region of $\delta = 2.60\text{--}0.70$, but splits when the temperature is decreased to -40°C to give rise to a new signal at -0.42 whose intensity corresponds to one proton. Stabilization of the vacant site by coordination of the BF_4^- counterion could be ruled out by the IR spectrum of **6**. It shows only one intense $\nu(\text{BF})$ band at 1060 cm^{-1} typical of noncoordinated BF_4^- .^[18]

X-ray structure analysis of $[\{\text{Rh}(\text{CO})(\text{S}_4^{\text{bu}})\}_2](\text{BF}_4)_2 \cdot 8\text{CH}_2\text{Cl}_2$ ($5 \cdot 8\text{CH}_2\text{Cl}_2$): The molecular structure of the $[\{\text{Rh}(\text{CO})(\text{S}_4^{\text{bu}})\}_2]^{2+}$ cation of $5 \cdot 8\text{CH}_2\text{Cl}_2$ is depicted in Figure 4. Table 1 lists selected distances and angles.

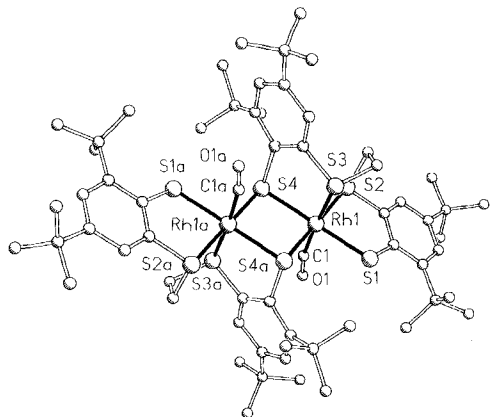


Figure 4. Structure of the $[\text{Rh}(\text{CO})(\text{S}_4^{\text{bu}})]_2^{2+}$ cation of $5 \cdot 8\text{CH}_2\text{Cl}_2$.

Table 1. Selected distances and angles in $[\{\text{Rh}(\text{CO})(\text{S}_4^{\text{bu}})\}_2](\text{BF}_4)_2 \cdot 8\text{CH}_2\text{Cl}_2$ ($5 \cdot 8\text{CH}_2\text{Cl}_2$).

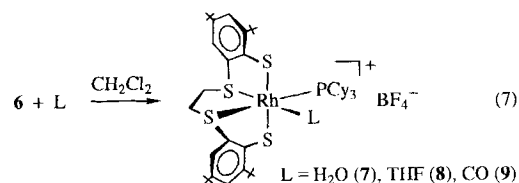
Distances [pm]		Angles [°]	
Rh(1)–S(1)	233.7(2)	S(1)–Rh(1)–S(2)	87.05(6)
Rh(1)–S(2)	233.2(2)	S(1)–Rh(1)–S(3)	91.36(6)
Rh(1)–S(3)	231.0(2)	S(1)–Rh(1)–S(4)	178.27(6)
Rh(1)–S(4)	237.0(2)	S(2)–Rh(1)–S(3)	89.36(7)
Rh(1)–S(4a)	242.0(2)	S(2)–Rh(1)–S(4)	93.71(6)
Rh(1)–C(1)	195.3(6)	S(1)–Rh(1)–S(4a)	92.66(6)
Rh(1)–Rh(1a)	349.0(2)	Rh(1)–S(4)–Rh(1a)	93.56(6)
C(1)–O(1)	111.0(8)	S(1)–Rh(1)–C(1)	84.6(2)

The complex **5** is the first $[\{M(\text{L})(\text{S}_4^{\text{bu}})\}_2]$ complex whose molecular structure could be determined by X-ray crystallography. The $[\{\text{Rh}(\text{CO})(\text{S}_4^{\text{bu}})\}_2]^{2+}$ cation of **5** consists of two enantiomeric $[\text{Rh}(\text{CO})(\text{S}_4^{\text{bu}})]^+$ fragments and possesses crystallographically required inversion symmetry. (According to the previously published stereochemical analysis of diastereomers that result from dimerization of chiral $[\text{M}(\text{L})(\text{S}_4^{\text{bu}})]$ fragments, the dication of **5** represents the α,α -*E(RS)* diastereomer.^[19])

Within each $[\text{Rh}(\text{CO})(\text{S}_4^{\text{bu}})]^+$ fragment, the distances between rhodium and nonbridging S donors, for example Rh(1)–S(1), Rh(1)–S(2), and Rh(1)–S(3), are nearly identical ($(\text{Rh}–\text{S})_{\text{av}} = 232.6(2)$ pm) and are typical of Rh–S (thioether or thiolate) distances.^[19, 20] The distances from rhodium to the bridging thiolate donors S(4) and S(4a) are significantly elongated (237.0(2) and 242.0(2) pm). The magnitude of these elongations contrasts with those found in most $[\{M(\text{L})(\text{S}_4^{\text{bu}})\}_2]$ complexes of the parent ligand “S₄”, which usually exhibit only slightly elongated M–S(thiolate)–M bridges.^[19] While the shorter Rh–S(bridge) distance (237.0(2) pm) can be traced back to the bridging function of the respective thiolate donor, the longer Rh–S(bridge) distance of 242.0(2) pm certainly indicates steric repulsion between the two $[\text{Rh}(\text{CO})(\text{S}_4^{\text{bu}})]^+$ fragments and a tendency of the dication of **5** to dissociate into monomers.

These results also support the assumption that the $[\text{Rh}(\text{PCy}_3)(\text{S}_4^{\text{bu}})]^+$ cation in **6** is mononuclear. When compared with the structure of **5**, the PCy₃ ligands of **6** recognizably increase the steric repulsion disfavoring dimerization. The long Rh(1)–C(1) (195.3(6) pm) and short C(1)–O(1) (111.0(8) pm) distances of **5** are also noteworthy. They indicate little Rh → CO π backbonding, and explain the ready dissociation of CO from **5** [cf. Eq. (5)].

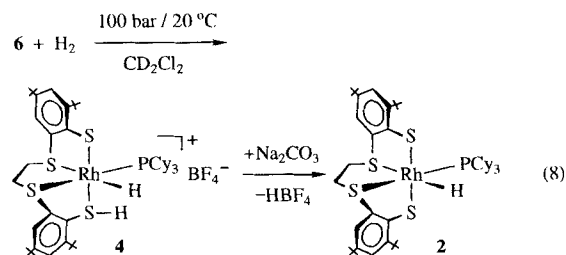
Coordination of H₂O, THF, and CO to $[\text{Rh}(\text{PCy}_3)(\text{S}_4^{\text{bu}})]\text{BF}_4$ (6**):** Complex **6** readily adds a sixth ligand such as L = H₂O, THF, or CO. The reactions are made visible by the color change of CH₂Cl₂ solutions of **6**, which turn from deep violet to red when L is added. The addition of H₂O or THF is reversible and yields the labile complexes $[\text{Rh}(\text{L})(\text{PCy}_3)(\text{S}_4^{\text{bu}})]\text{BF}_4$, L = H₂O (**7**) or THF (**8**), as set out in Equation (7). Evaporation of



the resultant solutions regenerated deep violet **6**. In contrast, CO adds irreversibly to form the stable CO complex $[\text{Rh}(\text{CO})(\text{PCy}_3)(\text{S}_4^{\text{bu}})]\text{BF}_4$ (**9**).

CD₂Cl₂ solutions of **7** exhibit a characteristic $\nu(\text{OH})$ IR band at 3502 cm⁻¹. The ¹H NMR spectrum of **7** in CD₂Cl₂ shows the typical pattern of the C₁ symmetrical $[\text{Rh}(\text{PCy}_3)(\text{S}_4^{\text{bu}})]^+$ fragment and, in addition, a broad singlet at $\delta = 3.95$ for the two H₂O protons. The $[\text{Rh}(\text{H}_2\text{O})(\text{PCy}_3)(\text{S}_4^{\text{bu}})]^+$ and $[\text{Rh}(\text{PCy}_3)(\text{S}_4^{\text{bu}})]^+$ ions could be detected in the mass spectra of the CD₂Cl₂ solutions. The ready coordination of H₂O by **6** was first noticed when elemental analyses of **6** were carried out. Correct elemental analyses could only be obtained for the adduct **6**·H₂O. The ¹H NMR spectrum of the analogous THF complex **8** (in CD₂Cl₂) revealed the typical two multiplets of THF at $\delta = 3.74$ and 1.83 which are shifted slightly downfield in comparison to uncoordinated THF ($\delta = 3.58$ and 1.73). The CO complex **9** was isolated in the solid state and characterized by elemental analyses and spectroscopic methods. Characteristic for **9** is its high-frequency $\nu(\text{CO})$ IR band at 2081 cm⁻¹ (in KBr).

Uptake and heterolysis of H₂ by **6 yielding $[\text{Rh}(\text{H})(\text{PCy}_3)(\text{S}_4^{\text{bu}})]\text{BF}_4$ (**4**):** Compound $[\text{Rh}(\text{PCy}_3)(\text{S}_4^{\text{bu}})]\text{BF}_4$ (**6**) also adds H₂. In this reaction the H₂ molecule is heterolytically cleaved, and the hydride thiol complex **4** forms according to Equation (8). The experiment was monitored by ¹H NMR spec-



troscopy. In a microautoclave, a CD_2Cl_2 solution of deep violet **6** was treated with 100 bar of H_2 for 5 h; a red solution resulted. The spectrum of this solution recorded at standard pressure proved the formation of **4** and minor amounts of by-products. When the reaction was carried out in the presence of solid Na_2CO_3 , a yellow solution was formed that contained the neutral hydride complex **2**. The formation of **2** is readily explained by deprotonation of the **4** that initially results [Eq. (8)].

Equation (8) suggests that the protonation of **2** by HBF_4 is reversible. This was examined and confirmed by an additional experiment showing that the red CH_2Cl_2 solution of **4** resulting from protonation of **2** by HBF_4 indeed yielded yellow **2** upon addition of solid Na_2CO_3 . The protonation of **2** by HBF_4 could also be reversed by addition of H_2O [acting as a Brønsted base; Eq. (9)].



Scrambling of thiol and hydride hydrogen atoms in $[\text{Rh}(\text{H})(\text{PCy}_3)(^{\text{bu}}\text{S}_4\text{-H})\text{BF}_4$ (4**) and $[\text{Rh}(\text{H})(\text{CO})(^{\text{bu}}\text{S}_4\text{-H})\text{BF}_4$ (**3**):** Intramolecular protonation of hydride ligands by thiol ligand protons is a reaction with very few precedents.^[1a, 8p, 9] When this reaction is reversible, scrambling of thiol protons and hydride ligands can be expected. Such a scrambling was observed when the deuterium-labeled derivatives $[\text{Rh}(\text{D})(\text{CO})(^{\text{bu}}\text{S}_4\text{-H})\text{BF}_4$ (**1a**) and $[\text{Rh}(\text{D})(\text{PCy}_3)(^{\text{bu}}\text{S}_4\text{-H})\text{BF}_4$ (**2a**) of **1** and **2** were protonated with HBF_4 . Complex **2a** was obtained from **1a** and PCy_3 by a synthesis analogous to that of **2**.^[10]

The protonation experiments were monitored by ^1H and ^2H NMR spectroscopy. CH_2Cl_2 , to which CD_2Cl_2 had been added as internal integration standard for the ^2H NMR measurements, served as solvent. For example, protonation of **2a** by HBF_4 led to a shift of the ^2H NMR deuteride signal to $\delta \approx -10.40$ and a decrease in its intensity of approximately 50%. Simultaneously, an SD signal of similar intensity appeared at $\delta = 5.80$ (Figure 5). The ^1H NMR spectrum of the same sample after protonation revealed a broad RhH signal at $\delta = -10.40$, which was identical to that observed for $[\text{Rh}(\text{H})(\text{PCy}_3)(^{\text{bu}}\text{S}_4\text{-H})\text{BF}_4$ (**4**). The intensity ratio of this signal to that of the aromatic protons was approximately 1:8 instead of 1:4 as in **4**.

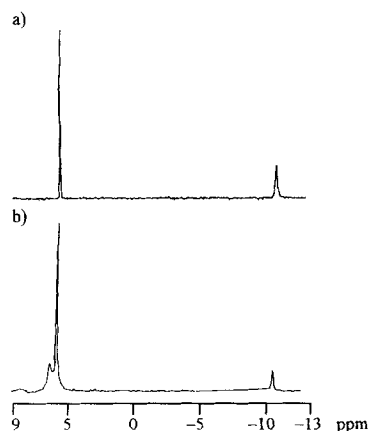
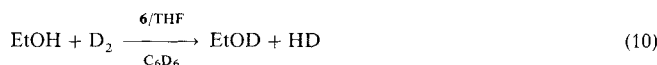


Figure 5. ^2H NMR spectra of a) $[\text{Rh}(\text{D})(\text{PCy}_3)(^{\text{bu}}\text{S}_4)]$ (**2**) and b) **2** after addition of HBF_4 (in methylene chloride, + 20 °C).

These results unambiguously demonstrate that protonation of the deuteride $[\text{Rh}(\text{D})(\text{PCy}_3)(^{\text{bu}}\text{S}_4)]$ (**2a**) by HBF_4 results not only in formation of the expected $[\text{Rh}(\text{D})(\text{PCy}_3)(^{\text{bu}}\text{S}_4\text{-H})\text{BF}_4$ but also in formation of deuterated thiol derivatives such as $[\text{Rh}(\text{D})(\text{PCy}_3)(^{\text{bu}}\text{S}_4\text{-D})\text{BF}_4$ as well as hydrides such as $[\text{Rh}(\text{H})(\text{PCy}_3)(^{\text{bu}}\text{S}_4\text{-D})\text{BF}_4$. The formation of these species requires an exchange (scrambling) between deuteride (hydride) ligands and thiol protons (deuterons).

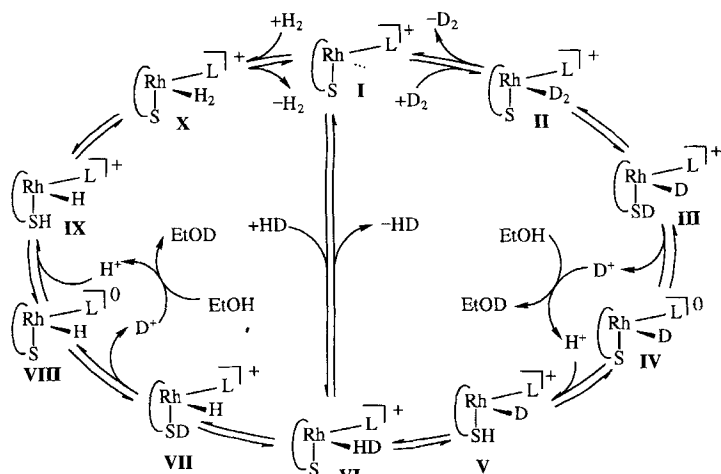
D_2/H^+ exchange catalyzed by $[\text{Rh}(\text{PCy}_3)(^{\text{bu}}\text{S}_4)]\text{BF}_4$: $[\text{Rh}(\text{PCy}_3)(^{\text{bu}}\text{S}_4)]\text{BF}_4$ (**6**) also catalyzes the D_2/H^+ exchange of Equation (10). In contrast to the D_2/H^+ exchange catalyzed by **1**, which requires the addition of catalytic amounts of HBF_4 , the catalysis in Equation (10) did not require the presence of Brønsted acids. This may be explained by the fact that **6** already possesses a vacant Rh site where D_2 may be added, whereas such a vacant site in **1** has first to be generated by attack of protons.



The catalysis described by Equation (10) was monitored by ^1H NMR and ^2H NMR spectroscopy and proved to exhibit a turnover number (TON) of only 7. This can be traced back to the relatively high stability of the hydride complexes **2** and **2a**. In fact, although it remained low, the TON could be doubled by addition of less than 1 equiv of HBF_4 , which partially converts **2**, via protonated **4** and release of H_2 , back into the catalytically active coordinatively unsaturated **6**. $^1\text{H}/^2\text{H}$ NMR spectroscopy further revealed that the reaction solution to which no HBF_4 had been added contained a 3:1 mixture of **2** and **2a**, but no **6**. This demonstrates that both species **2** and **2a** occur in the catalytic cycle and are more stable than coordinatively unsaturated **6**. In contrast, the catalysis reaction solution to which HBF_4 had been added contained a mixture of **2**, **2a**, and the protonated or deuterated derivatives, that is, **4** and its deuterated analogues resulting from protonation of **2** and **2a**.

Summarizing discussion of the mechanism of the D_2/H^+ exchange catalyzed by $[\text{Rh}(\text{L})(^{\text{bu}}\text{S}_4)]^+$ complexes: The rhodium complexes **1** and **2** have rendered possible the investigation of elementary reactions and the interception, isolation, and characterization of key intermediates of the D_2/H^+ exchange catalysis achieved with **1** and **2**. $[\text{Rh}(\text{H})(\text{PCy}_3)(^{\text{bu}}\text{S}_4)]$ (**2**), which is less labile than **1**, in some cases allowed observations that were not possible with **1**. The results obtained for **1** and **2** supplemented each other, yielded insight into the molecular mechanism of dihydrogen heterolysis at transition-metal sulfur sites, and allowed the D_2/H^+ exchange mechanism proposed for **1** to be described substantially in detail.^[9] The detailed mechanism is shown in Scheme 2.

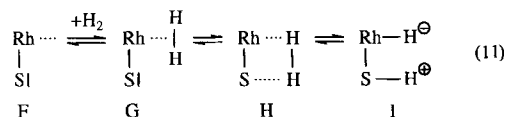
The cycle starts clockwise with the coordinatively unsaturated species **I**. Species **I** could be characterized as $[\text{Rh}(\text{PCy}_3)(^{\text{bu}}\text{S}_4)]\text{BF}_4$ (**6**) and probably occurs also as $[\text{Rh}(\text{CO})(^{\text{bu}}\text{S}_4)]^+$, as indicated by the molecular structure of $\{[\text{Rh}(\text{CO})(^{\text{bu}}\text{S}_4)]_2\}(\text{BF}_4)_2$ (**5**). The next step is D_2 addition to **I** to give **II**, which corresponds to **VI** and **X**. These species are the only ones that could not be characterized, so it remains open whether **II**, and **VI** and **X**, are actual intermediates or represent only transi-



Scheme 2. D_2/H^+ exchange catalyzed by $[Rh(H)(L)(^{*bu}S_4)]$ ($L = CO$ (**1**), PCy_3 (**2**)).

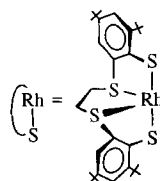
tion states. However, the next species, **III**, which corresponds to **IX**, **V**, and **VII**, could be proved to exist by the reaction of **6** with H_2 according to Equation (8). Species **III** releases its thiol deuteron, which exchanges with protons from EtOH. The exchangeability of the thiol deuterons and the formation of neutral **IV** follow from Equation (8) (deprotonation of **4** by Na_2CO_3) and from Equation (9) (reversibility of protonation of **2**). Neutral **IV** has been isolated as $[Rh(D)(L)(^{*bu}S_4)]$ ($L = CO$ (**2a**), PCy_3 (**4a**)). The protons from EtOH protonate neutral **IV** to give the thiol deuteride **V**. Species **V**, which corresponds to **VII**, **III**, and **IX**, follows from the protonation experiments of $[Rh(D)(L)(^{*bu}S_4)]$ ($L = CO$ (**1a**), PCy_3 (**2a**)) with HBF_4 . The NMR results prove that thiol protons and hydride ligands are scrambled in $[Rh(H)(L)(^{*bu}S_4-H)]BF_4$ complexes. Proton/deuteride scrambling leads from **V** to **VII** via **VI**. Species **VI** corresponds to **II** and cannot be described in detail. The consecutive steps **VII** \rightarrow **VIII** \rightarrow **IX** \rightarrow **X** \rightarrow **I** correspond to the steps **III** \rightarrow **IV** \rightarrow **V** \rightarrow **VI** \rightarrow **I**. Release of HD from **VI** completes the cycle to reform **I**.

The essential features of the catalysts and catalytic cycle are the Lewis-acidic vacant site at the rhodium center, the Brønsted-basic thiolate donors, and the reversibility of the individual reaction steps. Detection of the thiol hydride species **III**, **V**, **VII**, and **IX** and the scrambling of protons and hydride ligands further strongly indicate that the heterolytic cleavage of H_2 at the rhodium thiolate sites proceeds by an intramolecular mechanism. Thus, all observations are compatible with the four-center heterolysis mechanism indicated by species **H** in Equation (11).

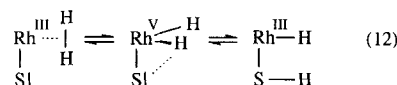


Intermediate or transient formation of the η^2-H_2 species **G** initiates the interaction between the Rh–S site and the H_2 molecule and allows the scrambling of thiol protons and hydride ligands via rotation of the H_2 molecule.

Alternative mechanisms that can be discussed for the scrambling of thiol protons and hydride ligands all require additional



assumptions and/or conflict with chemical experience. For example, the alternative of Equation (12) re-



quires the extra assumption of an oxidative addition of H_2 that, furthermore, is less likely when the metal

center is in medium or higher oxidation states. Another alternative mechanism for the scrambling of thiol protons and hydride ligands by conversion of the hydride ligand into a (second) thiol proton [Eq. (13)] requires the formation of a Rh^I center. In the case of $[RhH(PCy_3)(^{*bu}S_4-H)]^+$, the complex $[Rh(PCy_3)(^{*bu}S_4-H_2)]^+$ with a five coordinate Rh^I center and an 18-valence-electron configuration would result. For Rh^I , however, square-planar four-coordinate complexes with 16-valence-electron configurations are favored.

Relationships to other systems effecting heterolytic H_2 cleavage:

Heterolytic activation of H_2 by transition-metal complexes is well documented.^[1e] In many η^2-H_2 complexes,^[1, 5c] the η^2-H_2 ligand is rather acidic and forms classical hydrides by proton abstraction through intermolecular attack of bases.^[1a, 1d, 21] When these reactions are reversible, D_2/H^+ exchange catalysis has been proved to occur too, for example, with Ru and Os porphyrinato complexes,^[22] $[Ir(bq)(PPh_3)_2(H)(\eta^2-H_2)]-SbF_6$,^[21a] and $[Ru(dppe)_2(H)(\eta^2-H_2)]BF_4$.^[21a] Assistance by bases has also been observed in hydrogenation reactions catalyzed by $[Pd(salen)]$.^[23] The requirement for acids to achieve a D_2/H^+ exchange catalysis with the $[Rh(H)(L)(^{*bu}S_4)]$ complexes **1** and **2** is in merely superficial contrast to these findings. The acid is necessary only to generate vacant coordination sites at the Rh centers of **1** and **2**, and heterolytic H_2 cleavage leading to subsequent D_2/H^+ exchange can occur because **1** and **2** have thiolate donors as “built-in” bases.

Precedents for heterolytic H_2 cleavage by transition-metal centers carrying Brønsted-basic donors have been found in complexes such as $[Ir(CH_3)(I)\{N(SiMe_2CH_2PPh_2)_2\}]$ ^[24] and $[Ir(CH_3)(PPh_3)\{N(SiMe_2C_2PPh_2)_2\}]$,^[25] which contain amide and phosphide donors. These complexes, however, have not been reported to catalyze the D_2/H^+ exchange, which could be attributable to the fact that the amide and phosphide donors are stable only under aprotic conditions and not in H_2O or EtOH.

With regard to their transition-metal sulfur sites, the CpMo sulfide complexes reported by Rakowski Dubois et al. are more closely related to **1** and **2**. Complexes such as $[(\mu-S_2)(\mu-S)_2(MeCpMo)_2]$ add H_2 to give $[(\mu-SH)_2(\mu-S)_2(MeCpMo)_2]$. This reaction involves the cleavage of an S–S bond and does not appear to be reversible.^[26] It possibly comprises a reduction of the $[Mo_2(\mu-S_2)]$ entity accompanied by protonation of the resulting $\mu-S^{2-}$ ligands so that the reaction can be viewed as a coupled proton–electron transfer of the type proposed for Mo

enzymes.^[27] This would also explain why no formation of M–H groups could be found.

Reversible H₂ uptake with formation of S–H and M–H groups has been observed by Bianchini et al. with [(μ-S)₂{Rh(triphos)}₂]²⁺.^[28] This complex is also dinuclear and reacts with H₂ to give [(μ-SH)₂{Rh(H)(triphos)}₂]²⁺ (triphos = tris(methylenediphenylphosphine)methane), but the catalysis of D₂/H⁺ exchange has not been described.

D₂/H⁺-exchange catalysis and hydride–thiol proton scrambling have been described by Morris et al. for [Ir(H)₂(HS(CH₂)₃SH)(PCy₃)₂]BF₄.^[29] The mechanism proposed for the exchange processes compares with the one we have previously suggested for **1**^[9] and corroborated in this paper for **1** and **2**. The mechanism includes the intramolecular protonation of a hydride ligand by thiol protons and intermediate formation of an unobserved η²-H₂ complex. Disregarding the different metals and ligands and stressing the transition-metal sulfur site, **3**, **4**, and [Ir(H)₂(HS(CH₂)₃SH)(PCy₃)₂]BF₄ exhibit the same reactivity. The complexes differ in that **3** and **4** made possible the isolation of the neutral hydrides **1** and **2**, and also of the coordinatively unsaturated key intermediate [Rh(PCy₃)(^{bu}S₄)]BF₄ (**6**) as the actual catalyst for the D₂/H⁺-exchange catalysis. In this context, reference should be made to the pyridine-2-thiolate and quinoline-8-thiolate (quS) ruthenium and osmium complexes reported by Morris and co-workers.^[8p,q] For example, [Os(H)(CO)(quS)(PPh₃)₂] results in [Os(η²-H₂)(CO)(quS)(PPh₃)₂]⁺ and the tautomeric hydride thiol complex [Os(H)(CO)(quS-H)(PPh₃)₂]⁺, which are in temperature-dependent equilibrium. This equilibrium is explained most plausibly by hydride–thiol proton scrambling. Release of H₂ from these complexes leads to complete decomposition of the samples.

Catalysis of heterolytic H₂ cleavage is one of the characteristic reactivity features of hydrogenases whose active centers contain nickel–iron sulfur or iron sulfur sites. The physiological role of hydrogenases is the catalysis of the 2H⁺ + 2e⁻ ⇌ H₂ redox equilibrium [Eq. (1a)], but the D₂/H⁺-exchange catalysis is a suitable test reaction for determining the relevance of transition-metal complexes as models for hydrogenases. The [Rh(L)(^{bu}S₄)]⁺ complexes contain the biologically irrelevant rhodium, but they feature transition-metal sulfur centers that exhibit Lewis-acidic metal and Brønsted-basic thiolate sites. These two properties have been found to be essential requirements for the catalytic D₂/H⁺ exchange, so that the results obtained for rhodium sulfur sites may also hold for the nickel–iron sulfur sites of hydrogenase.

Conclusion

[Rh(L)(^{bu}S₄)]⁺ complexes featuring transition-metal sulfur sites with vacant coordination sites at the metal and Brønsted-basic sites at the thiolate donors have been found to catalyze heterolytic cleavage of dihydrogen and D₂/H⁺ exchange under ambient conditions. Isolation and characterization of key intermediates such as the coordinatively unsaturated [Rh(L)(^{bu}S₄)]⁺ species, the thiol hydride, and neutral hydride derivatives, and the observation of thiol proton and hydride scrambling, have yielded a detailed insight into the mechanism of the

heterolytic cleavage of dihydrogen at transition-metal sulfur sites. The uptake of dihydrogen by such sites probably proceeds via a η²-H₂ complex which is a transient state only and reversibly yields the thiol hydride species.

Experimental Section

General: Unless noted otherwise, all reactions and spectroscopic measurements were carried out at room temperature in freshly distilled solvents under an Ar atmosphere by standard Schlenk techniques, and the reactions were monitored by IR or NMR spectroscopy as far as possible; solvents were distilled before use over the appropriate drying agents. IR spectra of solutions were recorded in CaF₂ cuvettes with compensation of the solvent bands; solids were measured as KBr pellets or Nujol mull. Physical measurements were carried out with the following instruments: IR: Perkin–Elmer 983, Perkin–Elmer 1600 FTIR, and Perkin–Elmer 16PC FTIR. NMR: Jeol FT-JNM-GX270 and EX270, Jeol PMX 60SI. MS: Varian MAT 212.

DCl (38% in D₂O) was purchased from Fluka, HBF₄ (54% in ether) from Merck–Schuchardt, PPh₃ from Aldrich, and D₂ (99.9%) from Linde. RhCl₃·3H₂O was donated by Degussa. [Rh(H)(CO)(^{bu}S₄)] (**1**),^[9] [Rh(H)(PCy₃)(^{bu}S₄)] (**2**),^[10] and PCy₃^[30] were prepared as described in the literature. [Rh(D)(CO)(^{bu}S₄)]·THF (**1b**·THF)^[9] was dissolved in *n*-hexane and evaporated to dryness several times to remove residual THF, which is liable to influence protonation reactions with strong acids. ^{bu}S₄·D₂ was obtained from ^{bu}S₄·H₂^[31] dissolved in a mixture of a tenfold molar excess of two deuterated hydrochloric acid (38%) and THF, stirred for 2 h, and evaporated to dryness; this procedure was repeated three times.

Protonation of [Rh(H)(CO)(^{bu}S₄)] with HBF₄ to form [Rh(H)(CO)(^{bu}S₄-H)]BF₄ (**3**):

a) *Monitoring by ¹H NMR spectroscopy at -50 °C:* HBF₄ (3 μL, 0.023 mmol) was added to a light yellow solution of **1** (15 mg, 0.023 mmol) in 0.7 mL of CD₂Cl₂ at -50 °C. ¹H NMR (269.6 MHz, CD₂Cl₂): δ = 7.57 (s, 2H, C₆H₂), 7.46 (s, 1H, C₆H₂), 7.37 (s, 1H, C₆H₂), 3.50 (d, 1H, C₂H₄), 3.29 (d, 1H, C₂H₄), 2.70–2.53 (m, 1H, C₂H₄), 2.14–1.93 (m, 1H, C₂H₄), 1.56 (s, 18H, C₄H₉), 1.32 (s, 9H, C₄H₉), 1.26 (s, 9H, C₄H₉), -9.38 (brs, 1H, RhH).

b) *Monitoring by IR spectroscopy and isolation of products at -50 °C:* HBF₄ (6 μL, 0.05 mmol) was added to a light yellow solution of **1** (60 mg, 0.10 mmol) in 3 mL of CH₂Cl₂ at -78 °C. The IR spectrum of the solution was recorded at -70 °C and showed three characteristic bands in the ν(SH)/ν(CO)/ν(RhH) region at $\tilde{\nu}$ = 2482 cm⁻¹ (vw (broad), ν(SH)), [Rh(H)(CO)(^{bu}S₄-H)]BF₄ (**3**), 2110 (s, ν(CO), **3**), 2079 (s, ν(CO), **1**), 2000 (vw (broad), ν(RhH), **1** and **3**). After 1 h at -78 °C, an additional 6 μL of HBF₄ (0.05 mmol) was added, the IR spectrum was recorded ($\tilde{\nu}$ = 2482 cm⁻¹ (vw (broad), ν(SH), **3**), $\tilde{\nu}$ = 2110 cm⁻¹ (vs, ν(CO), **3**), 1992 (vw (broad), ν(RhH), **3**)).

c) *Protonation at room temperature:* HBF₄ (20 μL, 0.15 mmol) was added to a yellow solution of **1** (100 mg, 0.15 mmol) in 4 mL of CH₂Cl₂ at ambient temperatures. Gas was evolved, and the color of the solution changed to dark red. The gas was determined volumetrically with a gas burette at 20 °C (0.28 mmol after 5 h) and identified as a mixture of H₂ and CO by gas chromatography.

Protonation of [Rh(H)(PCy₃)(^{bu}S₄)] (**2**) with HBF₄ forming [Rh(H)(PCy₃)(^{bu}S₄-H)]BF₄ (**4**):

a) *Monitoring by ¹H NMR spectroscopy at temperatures between +30 °C and -90 °C:* HBF₄ (3 μL, 0.023 mmol) was added to a yellow solution of **2** (21 mg, 0.023 mmol) in 0.7 mL of CD₂Cl₂ in an NMR tube. ¹H NMR spectra of the resulting dark red solution were recorded at various temperatures. ¹H NMR (269.6 MHz, CD₂Cl₂): +30 °C: δ = 7.50 (brs, 3H, C₆H₂), 7.37 (s, 1H, C₆H₂), 5.5 (very brs, 1H, SH), 3.37–3.20 (m, 2H, C₂H₄), 2.60–0.72 (m, 33H, P(C₆H₁₁)₃; 2H, C₂H₄; superimposed), 1.59 (s, 9H, C₄H₉), 1.57 (s, 9H, C₄H₉), 1.31 (s, 9H, C₄H₉), 1.28 (s, 9H, C₄H₉), -10.40 (brs, 1H, RhH); +20 °C: δ = 7.50 (brs, 3H, C₆H₂), 7.37 (s, 1H, C₆H₂), 5.5 (brs, 1H, SH), 3.27 (brs, 2H, C₂H₄), 2.60–0.70 (m, 33H, P(C₆H₁₁)₃; 2H, C₂H₄; superimposed), 1.59 (s, 9H, C₄H₉), 1.57 (s, 9H, C₄H₉), 1.31 (s, 9H, C₄H₉), 1.28 (s, 9H, C₄H₉), -10.30 (brs, 1H, RhH); -20 °C: δ = 11.02 (brs, 0.25H,

SH), 8.23 (brs, 0.05H, *SH*), 5.87 (brs, 0.35H, *SH*), 5.35 (brs, 0.35H, *SH*), 7.90–7.10 (m, 4H, C_6H_2), 3.35–(–0.30) (m, 33H, $P(C_6H_{11})_3$); 4H, C_2H_4 ; superimposed), –9.89 (brs, 0.7H, *RhH*), –10.81 (brs, 0.3H, *RhH*); –90 °C: δ = 11.67 (brs, 0.25H, *SH*), 10.32 (brs, 0.05H, *SH*), 5.90 (brs, 0.35H, *SH*), 5.35 (brs, 0.35H, *SH*), 7.90–7.10 (m, 4H, C_6H_2), 3.60–(–0.80) (m, 33H, $P(C_6H_{11})_3$); 4H, C_2H_4 ; superimposed), –9.75 (pseudo-t, 0.35H, *RhH*, $^1J(RhH) = ^2J(PH) = 12$ Hz), –9.85 (pseudo-t, 0.35H, *RhH*, $^1J(RhH) = ^2J(PH) = 12$ Hz), –10.34 (pseudo-t, 0.05H, *RhH*, $^1J(RhH) = ^2J(PH) = 12$ Hz), –10.87 (pseudo-t, 0.25H, *RhH*, $^1J(RhH) = ^2J(PH) = 12$ Hz).

b) **Monitoring by IR spectroscopy and isolation of [Rh(PCy₃)(^{bu}S₄)]BF₄ (6):** HBF₄ (0.072 mL, 0.53 mmol) was added dropwise to a yellow solution of **2** (485 mg, 0.53 mmol) in 5 mL of CH₂Cl₂. The resulting dark red solution revealed two characteristic IR bands at $\tilde{\nu} = 2459$ (w, $\nu(SH)$) and 2032 cm^{–1} (w, $\nu(RhH)$) that slowly decreased in intensity in the course of 1 h. After 1 h the solution was evaporated to dryness, and the resultant deep violet residue was dried in vacuo. Yield: 520 mg **6** (98%). ¹H NMR (269.6 MHz, CD₂Cl₂): δ = 7.52 (s, 1H, C_6H_2), 7.49 (s, 1H, C_6H_2), 7.45 (s, 1H, C_6H_2), 7.10 (s, 1H, C_6H_2), 3.10 (d, 1H, C_2H_4), 2.98 (d, 1H, C_2H_4), 2.95–2.82 (m, 1H, C_2H_4), 2.60–0.70 (m, 33H, $P(C_6H_{11})_3$); 1H, C_2H_4 ; superimposed), 1.66 (s, 18H, C_4H_9), 1.33 (s, 9H, C_4H_9), 1.28 (s, 9H, C_4H_9); ³¹P{¹H} NMR (109.38 MHz): δ = 40.5 (d, $^1J(RhP) = 113.0$ Hz); IR (CH₂Cl₂): $\tilde{\nu} = 1060$ cm^{–1} (vs (broad), $\nu(BF)$); MS (FD, CH₂Cl₂): *m/z*: 915 ([Rh(PCy₃)(^{bu}S₄)])⁺, 887 ([Rh(PCy₃)(^{bu}S₂)₂])⁺. In the solid state (at standard pressure), complex **6** was extremely hygroscopic and correct elemental analyses could only be obtained for the H₂O adduct [Rh(H₂O)(PCy₃)(^{bu}S₄)]BF₄ (**7**) (see text and below). C₄₈H₇₇BF₄PRhS₄·H₂O (1021.09): calcd C 56.50, H 8.04, S 12.50; found C 56.46, H 7.80, S 12.56.

[Rh(H₂O)(PCy₃)(^{bu}S₄)]BF₄ (7): H₂O (0.93 μ L, 0.05 mmol) was added to a violet solution of **6** (52 mg, 0.05 mmol) in 0.7 mL of CD₂Cl₂. Spectra of the resulting dark red solution were recorded after 10 min. ¹H NMR (269.6 MHz, CD₂Cl₂): δ = 7.47 (s, 1H, C_6H_2), 7.43 (s, 2H, C_6H_2), 7.07 (s, 1H, C_6H_2), 3.95 (brs, 2H, H₂O), 3.05 (d, 1H, C_2H_4), 2.92–2.65 (m, 2H, C_2H_4), 2.55–0.70 (m, 33H, $P(C_6H_{11})_3$); 1H, C_2H_4 ; superimposed), 1.65 (s, 18H, C_4H_9), 1.30 (s, 9H, C_4H_9), 1.25 (s, 9H, C_4H_9); ³¹P{¹H} NMR (109.38 MHz, CD₂Cl₂): δ = 31.6 (d, $^1J(RhP) = 105$ Hz); IR (CD₂Cl₂): $\tilde{\nu} = 3502$ cm^{–1} (m (broad), $\nu(OH)$), $\tilde{\nu} = 1620$ cm^{–1} (m (broad), $\delta(OH_2)$), 1061 (sst (broad), $\nu(BF)$); MS (FD, CD₂Cl₂): *m/z*: 933 ([Rh(H₂O)(PCy₃)(^{bu}S₄)])⁺, 915 ([Rh(PCy₃)(^{bu}S₄)])⁺.

[Rh(THF)(PCy₃)(^{bu}S₄)]BF₄ (8): THF (3.0 μ L, 0.038 mmol) was added to a violet solution of **6** (38 mg, 0.038 mmol) in 0.7 mL of CD₂Cl₂. A ¹H NMR spectrum of the resulting dark red solution was recorded after 10 min. ¹H NMR (269.6 MHz, CD₂Cl₂): δ = 7.53 (s, 1H, C_6H_2), 7.49 (s, 1H, C_6H_2), 7.44 (s, 1H, C_6H_2), 7.10 (s, 1H, C_6H_2), 3.74 (brs, 4H, $C_2H_2C_2H_2O$), 3.20–2.85 (m, 3H, C_2H_4), 2.55–0.70 (m, 33H, $P(C_6H_{11})_3$); 1H, C_2H_4 ; superimposed), 1.83 (brs, 4H, $C_2H_4C_2H_4O$), 1.64 (s, 18H, C_4H_9), 1.32 (s, 9H, C_4H_9), 1.18 (s, 9H, C_4H_9).

[Rh(CO)(PCy₃)(^{bu}S₄)]BF₄ (9): CO was bubbled through a violet solution of **6** (100 mg, 0.10 mmol) in 10 mL of CH₂Cl₂ for 3 min. The resulting orange solution was evaporated to dryness, and the orange residue was dried in vacuo. Yield: 105 mg [Rh(CO)(PCy₃)(^{bu}S₄)]BF₄·0.5CH₂Cl₂ (98%). ¹H NMR (269.6 MHz, CD₂Cl₂): δ = 7.48 (s, 2H, C_6H_2), 7.41 (s, 1H, C_6H_2), 7.30 (d, 1H, C_6H_2), 3.62 (d, 1H, C_2H_4), 3.36 (d, 1H, C_2H_4), 3.07–2.93 (m, 1H, C_2H_4), 2.63–2.48 (m, 1H, C_2H_4), 2.47–0.85 (m, 33H, $P(C_6H_{11})_3$), 1.61 (s, 9H, C_4H_9), 1.59 (s, 9H, C_4H_9), 1.30 (s, 9H, C_4H_9), 1.28 (s, 9H, C_4H_9); ³¹P{¹H} NMR (109.38 MHz, CD₂Cl₂): δ = 46.3 (d, $^1J(RhP) = 91.0$ Hz); IR (KBr): $\tilde{\nu} = 2081$ cm^{–1} (vs, $\nu(CO)$), 1059 (vs (broad), $\nu(BF)$); MS (FD, CH₂Cl₂): *m/z*: 943 ([Rh(CO)(PCy₃)(^{bu}S₄)])⁺, 915 ([Rh(PCy₃)(^{bu}S₄)])⁺; C₄₉H₇₇BF₄OPRhS₄·0.5CH₂Cl₂ (1073.54): calcd C 55.98, H 7.81, S 11.48; found C 55.38, H 7.32, S 11.95.

[Rh(H)(PCy₃)(^{bu}S₄)] (2) and [Rh(H)(PCy₃)(^{bu}S₄)-H]BF₄ (4) from 6 and H₂: Two samples of **6** (42 mg, 0.042 mmol) were dissolved in 0.7 mL of CD₂Cl₂; Na₂CO₃ (3.60 mg, 0.042 mmol) was added to one of the resultant violet solutions (sample b), before both samples were placed in a microautoclave at 100 bar H₂ pressure for 5 days. NMR spectra of the resulting red (a) and yellow (b) solutions were recorded, proving the formation of **4** together with small amounts of byproducts (a) and the quantitative formation of **2** (b).

¹H NMR (269.6 MHz, CD₂Cl₂): (a): **4**, see above. (b): δ = 7.41 (d, 1H, C_6H_2), 7.33 (d, 1H, C_6H_2), 7.29–7.25 (m, 2H, C_6H_2), 3.17–3.00 (m, 2H, C_2H_4), 2.50–0.80 (m, 33H, $P(C_6H_{11})_3$); 2H, C_2H_4 ; superimp.), 1.63 (s, 9H, C_4H_9), 1.61 (s, 9H, C_4H_9), 1.30 (s, 9H, C_4H_9), 1.29 (s, 9H, C_4H_9), –11.02 (pseudo-t, 1H, *RhH*, $^1J(RhH) = ^2J(PH) = 13.1$ Hz).

Monitoring the protonation of 2 with HBF₄ and the subsequent deprotonation with water by ¹H NMR spectroscopy: HBF₄ (8.1 μ L, 0.059 mmol) was added to a yellow solution of **2** (54 mg, 0.059 mmol) in 0.7 mL of CD₂Cl₂ (a). The ¹H NMR spectrum (+ 20 °C) of the resultant dark red solution proved the formation of **4**. Degassed H₂O (10.8 μ L, 0.60 mmol) was added to the solution whose color turned from red to yellow. After stirring for 10 min and separation of the CD₂Cl₂ and H₂O phases, the ¹H NMR spectrum of the CD₂Cl₂ phase revealed the presence of **2** and an additional signal at δ = 5.09 resulting from excess H₂O.

[Rh(D)(PCy₃)(^{bu}S₄)] (2a): Solid PCy₃ (51 mg, 0.18 mmol) was added to a solution of [Rh(D)(CO)(^{bu}S₄)] (**1a**, 120 mg, 0.18 mmol) in 15 mL of *n*-hexane. Gas evolved, and the color of the solution changed from yellow to light orange. After 40 min, the solvent was removed in vacuo, and the yellow residue was dried in vacuo. Yield: 170 mg of **2a**·0.5*n*-hexane (98%). ¹H NMR (269.6 MHz, CD₂Cl₂): δ = 7.41 (d, 1H, C_6H_2), 7.33 (d, 1H, C_6H_2), 7.29–7.25 (m, 2H, C_6H_2), 3.17–3.00 (m, 2H, C_2H_4), 2.50–0.80 (m, 33H, $P(C_6H_{11})_3$); 2H, C_2H_4 ; superimposed), 1.63 (s, 9H, C_4H_9), 1.61 (s, 9H, C_4H_9), 1.30 (s, 9H, C_4H_9), 1.29 (s, 9H, C_4H_9); ²H NMR (41.25 MHz, CH₂Cl₂): δ = –10.96 (s, 1D, *RhD*); IR (KBr): $\tilde{\nu} = 1460$ cm^{–1} (w, $\nu(RhD)$); C₅₁H₈₄DPRhS₄ (961.37): calcd C 63.72, H 9.02, S 13.34; found C 63.83, H 8.95, S 13.39.

Protonation of [Rh(D)(L)(^{bu}S₄)] complexes with HBF₄ monitored by NMR spectroscopy:

a) **[Rh(D)(PCy₃)(^{bu}S₄)] (2a):** HBF₄ (4 μ L, 0.029 mmol) was added to a yellow solution of **2a** (27 mg, 0.029 mmol) in 0.7 mL of CH₂Cl₂ and 3.2 μ L (0.10 mmol) of CD₂Cl₂. ¹H and ²H NMR spectra of the resulting dark red solution were recorded. ¹H NMR (269.6 MHz, CH₂Cl₂, + 20 °C): δ = 7.50 (s, 3H, C_6H_2), 7.37 (s, 1H, C_6H_2), –10.40 (brs, \approx 0.5H, *RhH*); ²H NMR (41.25 MHz, CH₂Cl₂): δ = 5.80 (s, \approx 0.5D, *SD*), –10.40 (s, \approx 0.5D, *RhD*).

b) **[Rh(D)(CO)(^{bu}S₄)] (1a):** HBF₄ (4.7 μ L, 0.035 mmol) was added to a yellow solution of **1a** (23 mg, 0.035 mmol) in 0.7 mL of CH₂Cl₂ and 1.1 μ L (0.035 mmol) of CD₂Cl₂ at –50 °C. ¹H and ²H NMR spectra of the resulting light yellow solution were recorded. ¹H NMR (269.6 MHz, CH₂Cl₂): δ = 7.57 (s, 2H, C_6H_2), 7.46 (s, 1H, C_6H_2), 7.37 (s, 1H, C_6H_2), –9.40 (brs, 0.5H, *RhH*); ²H NMR (41.25 MHz, CH₂Cl₂): δ = –9.40 (s, 0.5D, *RhD*).

D₂/H⁺ exchange monitored by the formation of EtOD from EtOH and D₂ in the presence of 6: Two samples of complex **6** (30 mg, 0.030 mmol) were each dissolved in THF (0.93 mL) containing EtOH (0.047 mL, 0.79 mmol) and C₆D₆ (0.023 mL, 0.24 mmol). HBF₄ (3.7 μ L, 0.028 mmol) was added to one sample. The resultant red solutions were stored in a microautoclave under 60 bar D₂ pressure for 3 days. After release of the D₂ pressure, yellow solutions were obtained. The amount of resultant EtOD in these solutions was determined by ²H NMR spectroscopy (δ = 3.58); C₆D₆ (δ = 7.15) served as an internal reference and as a standard for the calculation of the turnover number (TON). The TON was 7 in the absence and 14 in the presence of HBF₄. Control experiments in the absence of **6** yielded no EtOD under otherwise identical conditions. The resultant reaction mixtures were identified by ¹H/²H NMR spectroscopy. The sample to which no HBF₄ had been added revealed the presence of [Rh(H)(PCy₃)(^{bu}S₄)] (**2**) and [Rh(D)(PCy₃)(^{bu}S₄)] (**2a**). The sample to which HBF₄ had been added contained **2**, **2a**, and protonated species, that is, **4** and its deuterated analogues.

X-ray structure analysis of {[Rh(CO)(^{bu}S₄)]₂(BF₄)₂·8CH₂Cl₂ (5)·8CH₂Cl₂: Black single crystals (blocks) of **5**·8CH₂Cl₂ were obtained from a solution of **1** (90 mg, 0.135 mmol) in CH₂Cl₂ (3 mL) which had been combined with HBF₄ (18 μ L, 0.135 mmol) at room temperature, and had subsequently been kept at –30 °C for one year. Table 2 contains selected crystallographic data for **5**·8CH₂Cl₂. A suitable single crystal of **5**·8CH₂Cl₂ was mounted on a Siemens P4 diffractometer. Data were collected with MoK α radiation (71.073 pm) in a 2 θ range of 3.0 to 54.0° with varying scan speed (3.00–29.30° min^{–1}) with the ω -scan technique. The structure was solved by direct methods (SHELXTL-PLUS).^[32] non-hydrogen atoms were refined

Table 2. Selected crystallographic data for $\{[\text{Rh}(\text{CO})(\text{C}^{\text{H}}\text{S}_4^{\text{H}})]_2(\text{BF}_4)_2 \cdot 8\text{CH}_2\text{Cl}_2 (5 \cdot 8\text{CH}_2\text{Cl}_2)$.

formula	$\text{C}_{70}\text{H}_{104}\text{B}_2\text{Cl}_{16}\text{F}_8\text{O}_2\text{Rh}_2\text{S}_8$
M_r (g mol^{-1})	2180.65
crystal size (mm^3)	$0.7 \times 0.7 \times 0.6$
crystal system	triclinic
space group	$P\bar{1}$
a (pm)	1048.2(4)
b (pm)	1430.0(5)
c (pm)	1785.7(7)
α ($^\circ$)	100.49(3)
β ($^\circ$)	102.92(3)
γ ($^\circ$)	103.68(3)
Z	1
V (nm^3)	2.456(2)
ρ_{calc} (g cm^{-3})	1.475
$F(000)$	1112
μ (cm^{-1})	9.95
T (K)	180(2)
measured reflections	13564
independent reflections	10754
observed reflections	6679
refined parameters	476
$R1$; $wR2$ (%)	0.0694; 0.2134

with anisotropic thermal parameters, refinement versus F^2 (SHELXL-93).^[33] Hydrogen atoms were localized in a difference Fourier synthesis and fixed at their positions with common isotropic thermal parameters. The crystal contained four molecules of CH_2Cl_2 per asymmetric unit, one of which was disordered. It was refined isotropically with split positions for one chlorine atom. The hydrogen atoms of the CH_2Cl_2 molecules were not found. Further details of the crystal structure investigation can be obtained from the Fachinformationszentrum Karlsruhe, D-76344 Eggenstein-Leopoldshafen (Germany), on quoting the depository number CSD-404603.

Acknowledgements: Financial support from the Deutsche Forschungsgemeinschaft and the Fonds der Chemischen Industrie and a gift of $\text{RhCl}_3 \cdot x\text{H}_2\text{O}$ from Degussa AG, Hanau (Germany), are gratefully acknowledged.

Received: June 4, 1997 F 714

- [1] a) P. G. Jessop, R. H. Morris, *Coord. Chem. Rev.* **1992**, *121*, 155–284; b) R. H. Crabtree, *Acc. Chem. Res.* **1990**, *23*, 95–101; c) J. C. Green, M. L. H. Green, in *Comprehensive Inorganic Chemistry, Vol. 4* (Eds.: J. C. Bailar, Jr., H. J. Emeléus, R. Nyholm, A. F. Trotman-Dickenson), Pergamon, Oxford, **1973**, pp. 355–452; d) D. M. Heinekey, W. J. Oldham, Jr., *Chem. Rev.* **1993**, *93*, 913–926; e) P. N. Brothers, *Progr. Inorg. Chem.* **1981**, *28*, 1–61; f) R. H. Morris, *Can. J. Chem.* **1996**, *74*, 1907–1915.
- [2] a) K. Schneider, D. S. Path, R. Cammack, *Biochim. Biophys. Acta* **1983**, *748*, 353–361; b) S. P. J. Albracht, H. L. Kalkmann, E. C. Slater, *Biochim. Biophys. Acta* **1983**, *724*, 309–316; c) J. LeGall, P. O. Ljungdahl, I. Moura, H. D. Peck, Jr., A. Xavier, J. J. G. Moura, M. Teixeira, B. H. Huynh, D. V. DerVartanian, *Biochim. Biophys. Res. Commun.* **1982**, *106*, 610–616.
- [3] a) R. Cammack, *Adv. Inorg. Chem.* **1992**, *38*, 281–322; b) A. F. Kolodziej, *Progr. Inorg. Chem.* **1994**, *41*, 493–597; c) *The Bioinorganic Chemistry of Nickel* (Ed.: J. R. Lancaster, Jr.), VCH, Weinheim, **1988**.
- [4] a) A. Volbeda, E. Garcin, A. L. de Lacey, V. M. Fernandez, M. Frey, J. C. Fontecilla-Camps, *J. Am. Chem. Soc.* **1996**, *118*, 12989–12996; b) A. Volbeda, M.-H. Charon, C. Piras, E. Hatchikian, M. Frey, J. C. Fontecilla-Camps, *Nature (London)* **1995**, *373*, 580–587.
- [5] a) R. H. Holm in *Biological Aspects of Inorganic Chemistry* (Eds.: A. W. Addison, W. R. Cullen, D. Dolphin, B. R. James), Wiley, New York, **1977**, pp. 71–112; b) R. H. Crabtree, *Inorg. Chim. Acta* **1986**, *125*, L7–L8; c) J. G. Kubas, *Acc. Chem. Res.* **1988**, *21*, 120–128.
- [6] a) R. R. Chianelli, M. Daage, M. J. Ledoux, *Adv. Catal.* **1994**, *40*, 177–232; b) *Hydrotreating Technology for Pollution Control* (Eds.: M. L. Occelli, R. R. Chianelli), Marcel Dekker, New York, **1996**.
- [7] a) S. Vasudevan, J. M. Thomas, C. J. Wright, C. Sampson, *J. Chem. Soc. Chem. Commun.* **1982**, 418–419; b) J. Polz, H. Zeilinger, B. Müller, H. Knozinger, *J. Catal.* **1989**, *120*, 22–28; c) N. Y. Topsoe, H. Topsoe, *ibid.* **1993**, *139*, 641–651; d) M. LaCroix, S. Yuan, M. Breysee, C. Doremieux-Morin, J. Fraissard, *ibid.* **1992**, *138*, 409–412.
- [8] For metal hydride complexes with at least one sulfur co-ligand see a) T. E. Burrow, N. J. Lazarowich, R. H. Morris, J. Lane, R. L. Richards, *Polyhedron* **1989**, *8*, 1701–1704; b) D. W. Stephen, *Inorg. Chem.* **1984**, *23*, 2207–2212; c) B. Chaudret, R. Poilblanc, *Inorg. Chim. Acta* **1979**, *34*, L209–L210; d) A. J. Blake, R. O. Gould, A. J. Holder, T. J. Hyde, G. Reid, M. Schröder, *J. Chem. Soc. Dalton Trans.* **1990**, 1759–1764; e) W. D. Lemke, K. E. Travis, N. E. Takvoryan, D. H. Busch, *Adv. Chem. Ser.* **1976**, *150*, 358–378; f) D. Sellmann, L. Zapf, *Z. Naturforsch. B* **1985**, *40*, 380–388; g) R. L. Richards, *Coord. Chem. Rev.* **1996**, *154*, 83–87; h) S. A. Wander, J. H. Reibenspies, J. S. Kim, M. Y. Darensbourg, *Inorg. Chem.* **1994**, *33*, 1421–1426; i) M. T. Ahmet, C. Lu, J. R. Dilworth, J. R. Miller, Y. Zheng, D. E. Hibbs, M. B. Hursthouse, K. M. A. Malik, *J. Chem. Soc. Dalton Trans.* **1995**, 3143–3164; j) J. R. Dilworth, A. J. Hutson, J. S. Lewis, J. R. Miller, Y. Zheng, Q. Chen, J. Zubieta, *J. Chem. Soc. Dalton Trans.* **1996**, 1093–1104; k) L. D. Field, T. W. Hambley, B. C. K. Yau, *Inorg. Chem.* **1994**, *33*, 2009–2017; l) T. Yoshida, T. Adachi, T. Ueda, T. Tanaka, F. Goto, *J. Chem. Soc. Chem. Commun.* **1990**, 342–343; m) T. Yoshida, T. Adachi, T. Tanaka, F. Goto, *J. Organomet. Chem.* **1992**, *428*, C12–C16; n) D. Sellmann, A. Fetz, M. Moll, F. Knoch, *Polyhedron* **1989**, *8*, 613–625; o) M. J. Albeniz, M. L. Buil, M. A. Esteruelas, A. M. Lopez, L. A. Oro, B. Zeier, *Organometallics* **1994**, *13*, 3746–3748; p) M. Schlaf, R. H. Morris, *J. Chem. Soc. Chem. Commun.* **1995**, 625–626; q) M. Schlaf, A. J. Lough, R. H. Morris, *Organometallics* **1996**, *15*, 4423–4436.
- [9] D. Sellmann, J. Käppler, M. Moll, *J. Am. Chem. Soc.* **1993**, *115*, 1830–1836.
- [10] D. Sellmann, G. H. Rackelmann, F. Heinemann, F. Knoch, M. Moll, *Inorg. Chim. Acta*, submitted for publication.
- [11] a) D. Sellmann, G. Mahr, F. Knoch, M. Moll, *Inorg. Chim. Acta* **1994**, *224*, 45–59; b) D. Sellmann, T. Becker, F. Knoch, *Chem. Eur. J.* **1996**, *2*, 1092–1098; c) D. Sellmann, J. Sutter, in *Sulfur Coordinated Transition Metal Complexes: Biological and Industrial Significance* (Eds.: E. I. Stiefel, K. Matsumoto), ACS Symp. Ser. **1996**, *653*, 101–116.
- [12] a) R. H. Crabtree, M. Lavin, *J. Chem. Soc. Chem. Commun.* **1985**, 1661–1662.
- [13] D. G. Hamilton, R. H. Crabtree, *J. Am. Chem. Soc.* **1988**, *110*, 4126–4133.
- [14] M. T. Bautista, K. A. Earle, P. A. Maltby, R. H. Morris, C. T. Schweitzer, A. Sella, *J. Am. Chem. Soc.* **1988**, *110*, 7031–7036.
- [15] D. Sellmann, R. Weiss, F. Knoch, M. Moll, *J. Organomet. Chem.* **1990**, *391*, 327–343.
- [16] D. Sellmann, W. Ludwig, G. Huttner, L. Zsolnai, *J. Organomet. Chem.* **1985**, *294*, 199–207.
- [17] D. Sellmann, T. Hofmann, F. Knoch, *Inorg. Chim. Acta* **1994**, *224*, 61–71.
- [18] a) K. Richter, E. O. Fischer, C. G. Kreiter, *J. Organomet. Chem.* **1976**, *122*, 187–196; b) W. Beck, K. Schloter, K. Urban, *Inorg. Synth.* **1990**, *28*, 5–15.
- [19] D. Sellmann, R. Weiss, F. Knoch, G. Ritter, J. Dengler, *Inorg. Chem.* **1990**, *29*, 4107–4114.
- [20] D. Sellmann, A. Fetz, M. Moll, F. Knoch, *J. Organomet. Chem.* **1988**, *355*, 495–511.
- [21] a) A. C. Albeniz, D. M. Heinekey, R. H. Crabtree, *Inorg. Chem.* **1991**, *30*, 3632–3635; b) G. Jia, R. H. Morris, *J. Am. Chem. Soc.* **1991**, *113*, 875–883; c) M. S. Chisen, D. M. Heinekey, *ibid.* **1990**, *112*, 5166–5175.
- [22] a) J. P. Collman, P. S. Wagenknecht, R. T. Hembre, N. S. Lewis, *J. Am. Chem. Soc.* **1990**, *112*, 1294–1297; b) J. P. Collman, P. S. Wagenknecht, N. S. Lewis, *ibid.* **1992**, *114*, 5665–5673.
- [23] a) G. Henrici-Olive, S. J. Olive, *J. Mol. Catal.* **1976**, 121–135; b) G. Henrici-Olive, S. J. Olive, *Angew. Chem.* **1974**, *86*, 561–562; *Angew. Chem. Int. Ed. Engl.* **1974**, *13*, 549–550.
- [24] a) M. D. Fryzuk, P. A. MacNeil, *Organometallics* **1986**, *5*, 2469–2476; b) M. D. Fryzuk, P. A. MacNeil, S. J. Rettig, *J. Am. Chem. Soc.* **1987**, *109*, 2803–2812.
- [25] M. D. Fryzuk, K. Bhangu, *J. Am. Chem. Soc.* **1988**, *110*, 961–963.
- [26] a) M. Rakowski DuBois, D. L. DuBois, M. C. VanDerveer, R. C. Haltiwanger, W. K. Miller, *J. Am. Chem. Soc.* **1980**, *102*, 7456–7461; b) M. Rakowski DuBois, B. Jagirdar, B. Noll, S. Dietz, in ref. [11 c], pp. 269–281.
- [27] a) E. I. Stiefel in ref. [11 c], pp. 2–38; b) E. I. Stiefel, *Proc. Natl. Acad. Sci. USA* **1973**, *70*, 988–993; c) E. I. Stiefel, J. K. Gardner, *J. Less-Common Metals* **1974**, *36*, 521–533.
- [28] a) C. Bianchini, C. Mealli, A. Meli, M. Sabat, *Inorg. Chem.* **1986**, *25*, 4617–4618; b) C. Bianchini, A. Meli, *ibid.* **1987**, *26*, 4268–4271.
- [29] P. G. Jessop, R. H. Morris, *Inorg. Chem.* **1993**, *32*, 2236–2237.
- [30] K. Issleib, A. Brack, *Z. Anorg. Allg. Chem.* **1954**, *277*, 258–270.
- [31] a) D. Sellmann, G. Freyberger, R. Eberlein, E. Böhlen, G. Huttner, L. Zsolnai, *J. Organomet. Chem.* **1987**, *323*, 21–35; b) D. Sellmann, W. Reisser, *Z. Naturforsch. B* **1984**, *39*, 1268–1275.
- [32] *SHELXTL-PLUS for Siemens Crystallographic Research Systems*, Release 421/V, Siemens Analytical X-Ray Instruments Inc., Madison (WI), **1990**.
- [33] G. M. Sheldrick, *SHELXL-93, Program for the Refinement of Crystal Structures*, University of Göttingen, **1993**.